FORMATION OF THE SHORT-LIVED RADIONUCLIDE ^{36}Cl IN THE PROTOPLANETARY DISK DURING LATE-STAGE IRRADIATION OF A VOLATILE-RICH RESERVOIR

Benjamin Jacobsen[1,2,6], Jennifer Matzel[2,3], Ian D. Hutcheon[2,3], Alexander N. Krot[4], Qing-Zhu Yin[1],
Kazuhide Nagashima[4], Erick C. Ramon[2], Peter K. Weber[2], Hope A. Ishii[3], and Fred J. Ciesla[5]
[1] Department of Geology, University of California, Davis, CA 95616, USA; jacobsen5@llnl.gov
[2] Glenn T. Seaborg Institute, Chemical Science Division, Lawrence Livermore National Laboratory, Livermore, CA 94550, USA
[3] Institute for Geophysics and Planetary Physics, Lawrence Livermore National Laboratory, Livermore, CA 94550, USA
[4] School of Ocean, Earth Science and Technology, Hawai'i Institute of Geophysics and Planetology, University of Hawai'i at Mānoa, Honolulu, HI 96822, USA
[5] Department of the Geophysical Sciences, University of Chicago, Chicago, IL 60637, USA

ABSTRACT

Short-lived radionuclides (SLRs) in the early solar system provide fundamental insight into protoplanetary disk evolution. We measured the ^{36}Cl–^{36}S-isotope abundance in wadalite (< 15 μm), a secondary chlorine-bearing mineral found in calcium–aluminum-rich inclusions (CAIs) in the Allende CV chondrite, to decipher the origin of the SLR ^{36}Cl ($\tau_{1/2} \sim 3 \times 10^5$ yr) in the early solar system. Its presence, initial abundance, and the noticeable decoupling from ^{26}Al raise serious questions about the origin of SLRs. The inferred initial ^{36}Cl abundance for wadalite, corresponding to a ^{36}Cl/^{35}Cl ratio of $(1.81 \pm 0.13) \times 10^{-5}$, is the highest ^{36}Cl abundance ever reported in any early solar system material. The high level of ^{36}Cl in wadalite and the absence of ^{26}Al (^{26}Al/^{27}Al $\leqslant 3.9 \times 10^{-6}$) in co-existing grossular (1) unequivocally support the production of ^{36}Cl by late-stage solar energetic particle irradiation in the protoplanetary disk and (2) indicates that the production of ^{36}Cl, recorded by wadalite, is unrelated to the origin of ^{26}Al and other SLRs (^{10}Be, ^{53}Mn) recorded by primary minerals of CAIs and chondrules. We infer that ^{36}Cl was largely produced by irradiation of a volatile-rich reservoir in an optically thin protoplanetary disk adjacent to the region in which the CV chondrite parent asteroid accreted while the Sun was a weak T Tauri star. Subsequently, ^{36}Cl accreted into the Allende CV chondrite together with condensed water ices.

Key words: astrochemistry – meteorites, meteors, meteoroids – nuclear reactions, nucleosynthesis, abundances – protoplanetary disks

1. INTRODUCTION

The origin of short-lived ($\tau_{1/2} < 5$ Myr) and now extinct radionuclides (^{10}Be, ^{26}Al, ^{36}Cl, ^{41}Ca, ^{53}Mn, ^{60}Fe, hereafter SLRs) is fundamental to understanding the formation of the early solar system as they provide a unique source of information about the astrophysical environment in which the solar system formed, as well as high-resolution chronology of early solar system events (McKeegan & Davis 2003; Wasserburg et al. 2006). The origin of SLRs in the early solar system, however, remains controversial (Wasserburg et al. 2006). The two main classes of models proposed—injection of SLRs from a stellar source (e.g., supernova, asymptotic giant branch star or Wolf–Rayet star) and solar energetic particle (SEP) irradiation of dust and gas near the proto-Sun—have widely different consequences for the expected occurrences and distribution of SLRs in the early solar system (Wasserburg et al. 2006; Huss et al. 2009; Shu et al. 2001; Leya et al. 2003; Gounelle et al. 2006; Goswami et al. 2001). SLRs produced by stellar nucleosynthesis and injected into the protosolar molecular cloud are expected to homogenize quickly in the solar nebula; as a result, variations in their relative abundances may be ascribed to the passage of time (Wasserburg et al. 2006; Boss 2008). In contrast, SLRs produced by SEP irradiation are more likely to be heterogeneously distributed, and variations in their relative abundances would reflect the local energetic particle environment (Wasserburg et al. 2006).

Recently, excesses of ^{36}S correlated with ^{35}Cl/^{34}S ratios were reported in sodalite ($Na_8Al_6Si_6O_{24}Cl_2$), a secondary mineral in calcium–aluminium-rich inclusions (CAIs) and chondrules from the Allende (CV) and Ningqiang (CV anomalous) carbonaceous chondrites (Lin et al. 2005; Hsu et al. 2006; Ushikubo et al. 2007). These studies provide clear evidence for in situ decay of ^{36}Cl in the early solar system; they also highlight the long-standing dichotomy between the two classes of models proposed to explain the origin of SLRs. Theoretical calculations of SLR production by SEP irradiation (Leya et al. 2003; Gounelle et al. 2006) show that the highest reported ^{36}Cl levels in sodalite (i.e., ^{36}Cl/^{35}Cl $\sim 5 \times 10^{-6}$; Lin et al. 2005; Hsu et al. 2006) are consistent with levels predicted for energetic particle irradiation of a reservoir with solar composition, but exceed by several orders of magnitude the values predicted for any stellar source (Wasserburg et al. 2006). This is consistent with astronomical observations of pre-main-sequence, solar-type stars that show powerful X-ray flares believed to be accompanied by intense fluxes of accelerated particles (Feigelson et al. 2002). The irradiation models predict that the production of ^{36}Cl by SEP irradiation would not occur in isolation but be coupled to the production of other SLRs such as ^{26}Al, ^{53}Mn, and ^{10}Be (Leya et al. 2003; Gounelle et al. 2006; Goswami et al. 2001). However, this prediction is inconsistent with the absence of ^{26}Al in sodalite containing large ^{36}S excesses (Lin et al. 2005; Hsu et al. 2006; Ushikubo et al. 2007). Moreover, high-precision ^{26}Al–^{26}Mg systematic of primary phases in chondrules from unmetamorphosed chondrites suggests that Earth, CAIs, and chondrules all formed from a reservoir with a homogeneous distribution of ^{26}Al, supporting its stellar origin (Villeneuve et al. 2009). These conflicting data underscore the importance of ^{36}Cl and its relationship to ^{26}Al for understanding the origin of SLRs in the early solar system. This issue can only be

---

[6] Current address: Glenn T. Seaborg Institute, Chemical Science Division, Lawrence Livermore National Laboratory, Livermore, CA 94550, USA.

resolved if we understand when, where, and how ^{36}Cl formed and was incorporated into primitive meteorites containing a wide spectrum of objects—CAIs, chondrules, and matrix.

2. SAMPLE DETAILS AND ANALYTICAL METHODS

To address this issue, we studied a coarse-grained igneous CAI AJEF from the Allende meteorite. Primary minerals in AJEF (anorthite, melilite, pyroxene, and spinel) define an internal ^{26}Al–^{26}Mg isochron with an initial ^{26}Al/^{27}Al ratio of ∼5 × 10^{-5} (Jacobsen et al. 2008). Melilite and anorthite are replaced by the co-existing secondary minerals, wadalite (Ca$_6$(Al,Si,Mg)$_7$O$_{16}$Cl$_3$) and grossular (Ca$_3$Al$_2$Si$_3$O$_{12}$) (Figure 1), in which ^{36}Cl–^{36}S and ^{26}Al–^{26}Mg-isotope systematics were measured, respectively. Wadalite is a chlorine-rich mineral recently described in the Allende CAIs (Ishii et al. 2010). The high chlorine (∼12 wt%) and very low sulfur content (≪0.01 wt%) make wadalite ideal for studies of the ^{36}Cl–^{36}S system. Wadalite occurs exclusively in igneous (Type B) CAI cores, whereas sodalite is present in the outer portions of the CAIs (Krot et al. 2010). In Type B CAIs such as AJEF, wadalite is closely associated with other secondary minerals, including grossular, monticellite, and wollastonite, occurring either as anhedral grains intergrown with secondary minerals replacing melilite or in veins cross-cutting melilite and anorthite (Ishii et al. 2010).

The isotope abundances of chlorine and sulfur in wadalite in AJEF were determined with the Lawrence Livermore National Laboratory *Cameca* NanoSIMS 50, a secondary ion mass spectrometer (SIMS) with nanometer scale spatial resolution. A primary Cs$^+$ beam of ∼19 pA and diameter of ∼300 nm was used. Depending upon the size of the wadalite grain, the primary beam was rastered over areas between 4 × 4 μm^2 and 20 × 20 μm^2 in size to produce quantitative secondary ion images (Figure 2). Due to the low ^{36}S$^-$ count rate, the background at mass 36 was carefully evaluated. Background was measured 0.014 atomic mass units (amu) below ^{36}S (35.967 amu) by changing the deflection plate voltage on the electron multiplier used for ^{36}S by 10 V (Nakashima et al. 2008). The mean background intensity for wadalite in these measurements, 0.005 counts per second (cps), is ∼4× lower than that for sodalite. A mass resolving power ($m/\Delta m$, where m is mass ^{36}S and Δm is the peak width at 10% peak height) of ∼3600 was used, sufficient to eliminate any contribution from ^{12}C$_3{}^-$ or ^{35}ClH$^-$ on ^{36}S$^-$, but not high enough to resolve potential interferences from doubly charged ^{35}Cl^{37}Cl^{2-} and ^{56}Fe^{16}O^{2-} species. To evaluate these potential interferences, we analyzed terrestrial wadalite with the same Cl content but much lower S and ∼10 times higher FeO contents than wadalite in AJEF. No signal beyond the analytical background was observed at 35.967 amu, placing an upper limit on any potential ^{35}Cl^{37}Cl^{2-} or ^{56}Fe^{16}O^{2-} interferences of <0.001 cps. We also carefully monitored and evaluated potential interferences from ^{24}Mg^{48}Ca^{2-}, ^{28}Si^{44}Ca^{2-}, ^{40}Ca^{16}O$_2{}^{2-}$ etc. and concluded these species can be excluded as sources of error in our ^{36}S$^-$ measurement. Even at Cl/S ratios about six times higher than in AJEF wadalite, no excesses at mass 36 beyond analytical error are observed in terrestrial wadalite, effectively ruling out any analytical artifact associated with ^{36}S measurement of AJEF wadalite. Measured ^{37}Cl$^-$/ ^{34}S$^-$ ion ratios were converted to atomic ratios with a relative sensitivity factor of 0.70 ± 0.14 (2σ), determined from measurements of terrestrial scapolite (Na,Ca)$_4$(Al$_3$Si$_9$O$_{24}$)Cl and hauynite (Na,Ca)$_{4-8}$Al$_6$Si$_6$(O,S)$_{24}$(SO$_4$,Cl)$_{1-2}$. This relative sensitivity factor is within uncertainty similar to the values
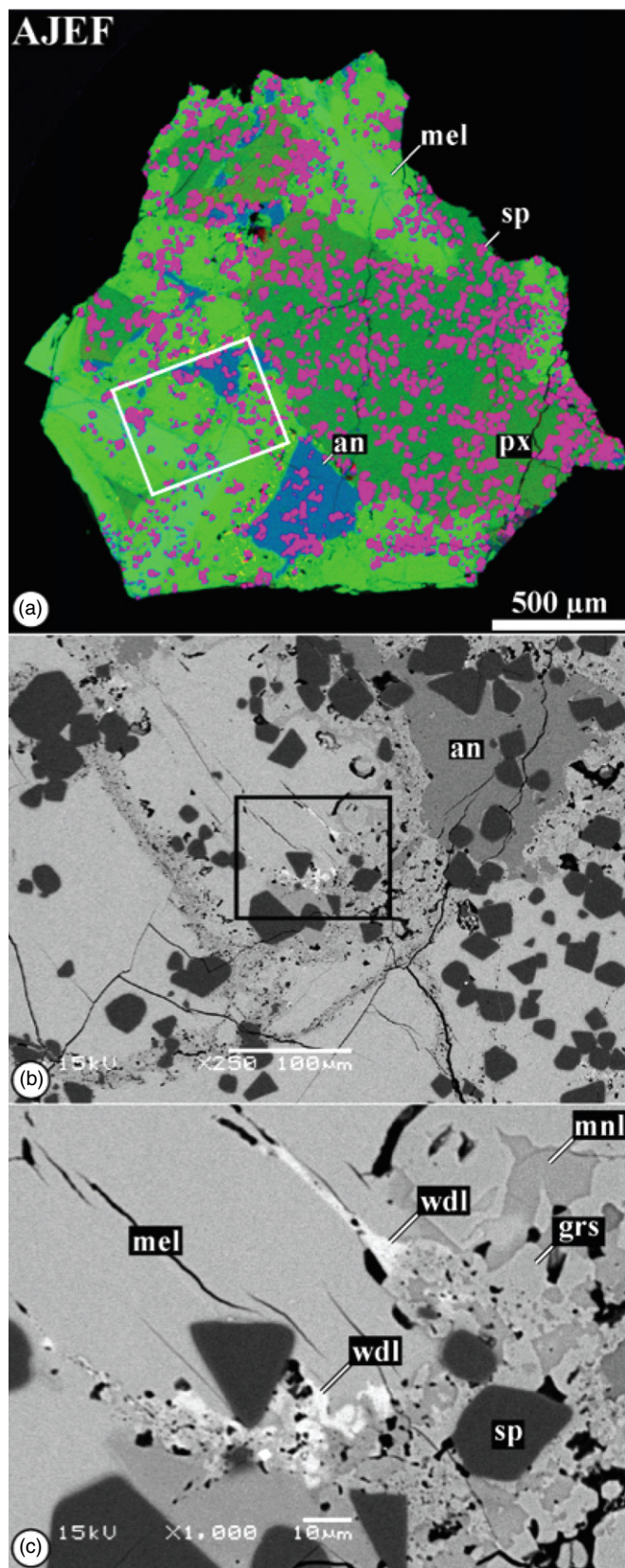

Figure 1. Combined X-ray elemental map in Mg (red), Ca (green), and Al (blue) (a) and backscattered electron images (b, c) of the wadalite-grossular paragenesis in the Allende Type B CAI AJEF. Regions outlined in panels (a) and (b) are shown in greater detail in panels (b) and (c), respectively. Wadalite together with grossular and monticellite occurs in secondary veins cross-cutting primary melilite. an = anorthite; grs = grossular; mel = melilite; mnl = monticellite; sp = spinel; wdl = wadalite.
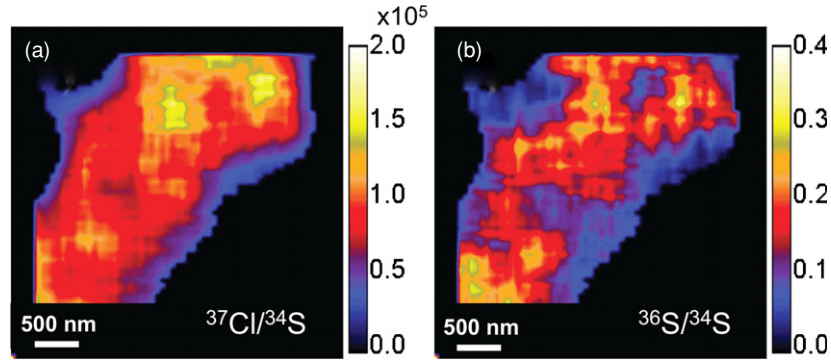
Figure 2. Example of a 4×4 μm NanoSIMS raster image of (a) $^{37}Cl/^{34}S$ and (b) the corresponding $^{36}S/^{34}S$ ratios as seen with the *LIMAGE* data processing software. This image corresponds to measurement 3 in Table 1. The red, orange, and yellow area is the wadalite grain.

Table 1
Sulfur Isotopic Compositions of Wadalite in the Allende CAI AJEF

Sample	$^{35}Cl/^{34}S$	$\delta^{36}S(‰)$	N
Terrestrial Minerals			
Scapolite...	1.18 ± 0.30	1 ± 128	5
	53 ± 17	1 ± 71	21
Hauynite...	1.82 ± 0.48	-18 ± 802	5
Sodalite...	1694 ± 327	0 ± 149	16
Wadalite...	$(2426 \pm 529) \times 10^3$	$(6 \pm 10) \times 10^3$	...
	$(10930 \pm 1364) \times 10^3$	$(0! \pm 34) \times 10^3$ [a]	...
Allende CAI–AJEF			
Wadalite 1...	$(1983 \pm 362) \times 10^3$	$(264 \pm 83) \times 10^3$	
	$(811 \pm 128) \times 10^3$	$(84 \pm 31) \times 10^3$	
	$(302 \pm 34) \times 10^3$	$(33 \pm 7) \times 10^3$	
	$(99 \pm 11) \times 10^3$	$(13 \pm 4) \times 10^3$	
	$(51.5 \pm 0.3) \times 10^3$	$(6 \pm 1) \times 10^3$	
Wadalite 2...	$(592 \pm 73) \times 10^3$	$(53 \pm 13) \times 10^3$	
	$(327 \pm 38) \times 10^3$	$(28 \pm 8) \times 10^3$	
	$(195 \pm 21) \times 10^3$	$(17 \pm 4) \times 10^3$	
	$(87 \pm 9) \times 10^3$	$(8 \pm 3) \times 10^3$	
	$(36 \pm 4) \times 10^3$	$(4 \pm 1) \times 10^3$	
	$(15 \pm 2) \times 10^3$	$(2 \pm 1) \times 10^3$	
	$(4.2 \pm 0.4) \times 10^3$	$(0.9 \pm 0.4) \times 10^3$	
Wadalite 3...	$(577 \pm 72) \times 10^3$	$(51 \pm 14) \times 10^3$	
	$(392 \pm 47) \times 10^3$	$(34 \pm 10) \times 10^3$	
	$(204 \pm 22) \times 10^3$	$(20 \pm 4) \times 10^3$	
	$(83 \pm 10) \times 10^3$	$(10 \pm 1) \times 10^3$	
Wadalite 4...	$(1328 \pm 365) \times 10^3$	$(146 \pm 78) \times 10^3$	
	$(548 \pm 131) \times 10^3$	$(91 \pm 50) \times 10^3$	
	$(266 \pm 35) \times 10^3$	$(27 \pm 6) \times 10^3$	

Notes. Errors are $2\sigma_{mean}$. N: number of repeat analyses for standards. To calculate the $^{36}S/^{34}S$ and $^{35}Cl/^{34}S$ ratios from the NanoSIMS images, we used the *LIMAGE* software, Larry Nittler (Carnegie Institution of Washington). *LIMAGE* extracts quantitative ion intensities and isotope ratios from NanoSIMS ion images. For each of the four image acquisitions, we created an internal data set by grouping individual pixels into sub-regions based on their $^{37}Cl/^{34}S$ ratios. It is thus possible to construct a regression line for each measurement, using different sub-regions with corresponding $^{35}Cl/^{34}S$ and $^{36}S/^{34}S$ ratios as individual data. Due to the low count rate on ^{36}S, the $^{35}Cl/^{34}S$ and $^{36}S/^{34}S$ ratios, for each sub-region, were calculated from the sum of the total counts of each isotope. Sulfur-isotope compositions are reported as parts per thousand (‰) deviation from the sulfur isotopic standard V-CDT, Canyon Diablo (IAB iron meteorite) troilite, with $^{36}S/^{34}S = 0.003475$ (Ding et al. 2001).
[a] $\delta^{36}S$ is denoted as "0!", as no counts above background were detected for ^{36}S.

reported for different Cl-rich minerals and standards, between 0.58 and 0.83 (Lin et al. 2005; Hsu et al. 2006; Ushikubo et al. 2007; Nakashima et al. 2008).

Magnesium-isotope compositions and $^{27}Al/^{24}Mg$ ratios of grossular, coexisting with wadalite, in AJEF were measured in situ with the *Cameca* ims 1280 ion microprobe at University of Hawai'i using a focused 5×7 μm primary $^{16}O^-$ ion beam. The mass resolving power was set to ~3800, sufficient to separate interfering hydrides and doubly charged $^{48}Ca^{2+}$. Instrumental mass fractionation was corrected by standard-sample bracketing by comparing each measurement with the isotope ratios measured in terrestrial grossular, assumed to have Mg-isotope
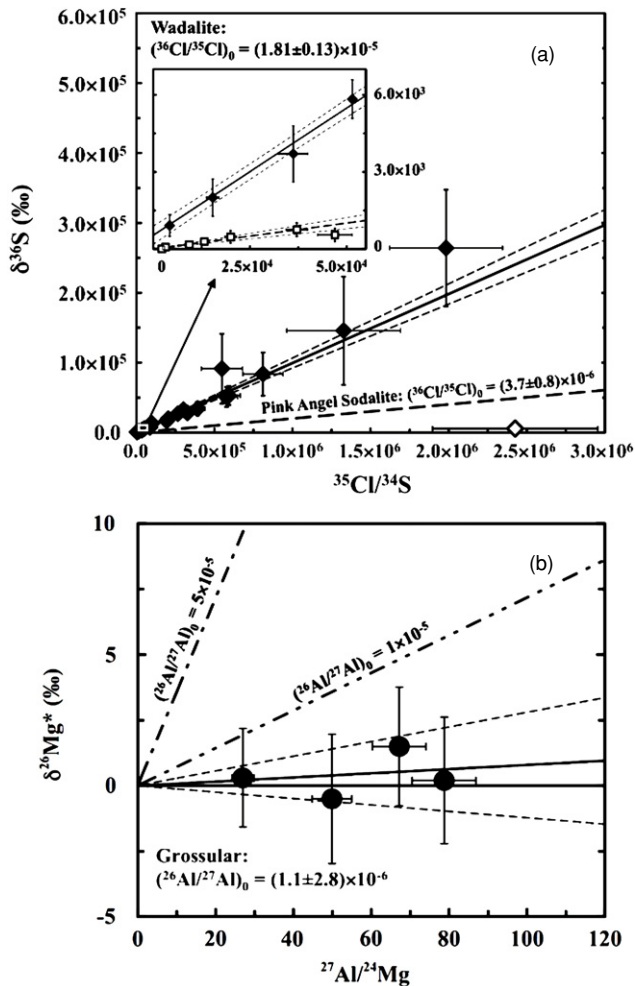
Figure 3. Panel (a): ^{36}Cl–^{36}S isochron diagram of wadalite from the Allende CAI AJEF (solid diamonds). The solid line represents a weighted, least-squares regression through the data and corresponds to $(^{36}Cl/^{35}Cl)_0 = (1.81 \pm 0.13) \times 10^{-5}$. Stippled lines represent the error envelope. The dashed line and lower slope in the inset represent the inferred $(^{36}Cl/^{35}Cl)_0$ ratio for sodalite (open squares) from the Allende CAI Pink Angel (Hsu et al. 2006). Terrestrial wadalite is shown as open diamond. Panel (b): ^{26}Al–^{26}Mg isochron diagram for grossular in the Allende CAI AJEF. The black solid line represents a weighted, least-squares regression through the data corresponding to $(^{26}Al/^{27}Al)_0 = (1.1 \pm 2.8) \times 10^{-6}$. Dashed lines represent the error envelope. The uncertainties in both panels (a) and (b) and inset are 2σ.

ratios as in Catanzaro et al. (1966). The $^{27}Al^+/^{24}Mg^+$ ratios were corrected using a sensitivity factor measured on a grossular standard, i.e., GRR1386, Lalatema Hills, and Tanzania.

3. TIMING OF ^{36}Cl PRODUCTION

The AJEF wadalite shows extremely large ^{36}S excesses with $^{36}S/^{34}S$ ratios of up to $\sim$264 times that of the Canyon Diablo troilite standard value, correlated with the respective $^{35}Cl/^{34}S$ ratios (as high as $\sim$2 × 10^6). The slope of a line fitted to the data yields an inferred $^{36}Cl/^{35}Cl$ ratio at the time of wadalite formation of $(1.81 \pm 0.13) \times 10^{-5}$ (Figure 3(a)). This value represents the highest initial abundance of ^{36}Cl reported in any meteorite and is more than four times greater than the highest $^{36}Cl/^{35}Cl$ initial ratio observed in sodalite in CAIs and chondrules (Lin et al. 2005; Hsu et al. 2006).

Grossular associated with wadalite shows no resolvable ^{26}Mg excess. The upper limit to the initial $^{26}Al/^{27}Al$ ratio in grossular is 3.9×10^{-6} (Figure 3(b)). This value is similar to the upper

limit obtained for sodalite in CV CAIs and chondrules (Lin et al. 2005; Hsu et al. 2006; Ushikubo et al. 2007). The absence of radiogenic ^{26}Mg in secondary grossular contrasts with the well-constrained primary mineral internal isochron in AJEF (Jacobsen et al. 2008) yielding an initial $^{26}Al/^{27}Al$ ratio of $\sim$5 × 10^{-5} and suggests that the wadalite-grossular paragenesis formed >2.6 Myr after crystallization of the CAI.

The well-defined ^{26}Al–^{26}Mg chronologies, for both primary and secondary minerals, within AJEF place important constraints on the origin of ^{36}Cl. If ^{36}Cl was produced together with ^{26}Al at the birth of the solar system, the late formation of wadalite inferred from the low $(^{26}Al/^{27}Al)_0$ ratio in co-genetic grossular, would require an unrealistically high initial $^{36}Cl/^{35}Cl$ ratio of >8.7 × 10^{-3} at the time the primary CAI mineral assemblage crystallized. This value is more than 60 times the maximum level that can be produced by SEP irradiation of gas and/or dust of solar composition (Leya et al. 2003; Gounelle et al. 2006). The high initial $^{36}Cl/^{35}Cl$ ratio in AJEF (1.8 × 10^{-5}) thus indicates that the production of ^{36}Cl by SEP irradiation must have occurred late, >2 Myr after the formation of the first solar system solids, and provides the first conclusive evidence that the ^{36}Cl found in secondary, low-temperature minerals in CAIs and chondrules was produced in processes unrelated to those responsible for the SLRs (^{26}Al, ^{41}Ca, ^{10}Be) observed in primary, high-temperature minerals in the same objects.

4. COLATERAL PRODUCTION OF SLRs DURING LATE-STAGE IRRADIATION

The suggestion that ^{36}Cl is produced by late-stage SEP irradiation must be evaluated against the predicted abundances of other SLRs and compared to the observed abundances in early solar system solids. Evidence for late-stage production of SLRs should be preserved in differentiated meteorites or in whole-rock samples of unequilibrated ordinary or carbonaceous chondrites. Assuming late-stage irradiation of a reservoir with solar composition and a particle fluence sufficient to produce ^{36}Cl corresponding to the inferred $^{36}Cl/^{35}Cl$ ratio in wadalite ($\sim$2 × 10^{-5}), we estimate, using the most recent calculations (Leya et al. 2003; Gounelle et al. 2006; Goswami et al. 2005), relative abundances of the co-produced ^{26}Al, ^{53}Mn, and ^{10}Be. The range in predicted abundances reflects different assumptions among the models regarding production cross sections, $^3He/H$ and $^3He/^4He$ ratios of SEP, hardness of the energy spectrum, and the relative importance of gradual to impulsive SEP events. The abundances of the three SLRs predicted here are compared against observed abundances in bulk meteorites (Thrane et al. 2006; Shukolyukov & Lugmair 2006; Moynier et al. 2007; Trinquier et al. 2008; see also Figure 4).

Evidence for late-stage production of ^{26}Al and ^{53}Mn, in the form of excesses of ^{26}Mg and/or ^{53}Cr, should be preserved in differentiated meteorites or in whole-rock samples of unequilibrated ordinary or carbonaceous chondrites. High-precision whole-rock magnesium-isotope measurements of chondrites and differentiated meteorites show that the abundance of radiogenic ^{26}Mg is < 5 ppm (Thrane et al. 2006). For a chondritic reservoir, assuming an initial $^{26}Al/^{27}Al$ ratio of 5 × 10^{-5}, this observation places an upper limit on the amount of ^{26}Al added by late-stage SEP irradiation corresponding to $^{26}Al/^{27}Al \leqslant 6 \times 10^{-6}$. The initial solar system abundance of ^{53}Mn is not well constrained; however, the amount of ^{53}Mn produced by late-stage SEP irradiation must be less than the observed levels of ^{53}Mn in carbonaceous chondrites (Shukolyukov & Lugmair
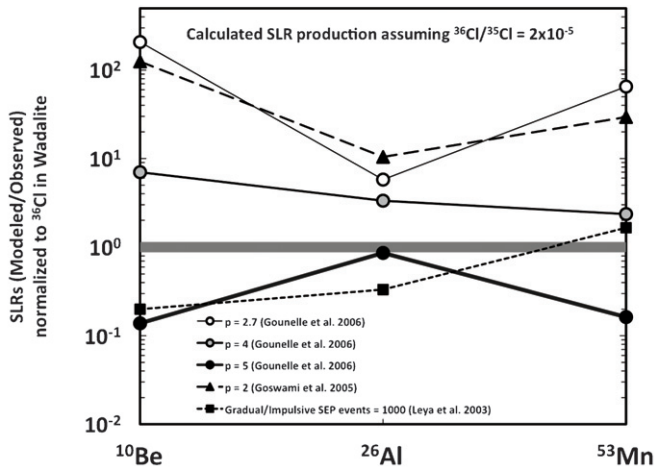
Figure 4. Ratio of calculated to observed abundances of ^{10}Be, ^{26}Al, and ^{53}Mn assuming a particle fluence sufficient to produce ^{36}Cl corresponding to $(^{36}$Cl/^{35}Cl$) = 2 \times 10^{-5}$. The calculated ^{26}Al and ^{53}Mn abundances are normalized to the inferred upper limits of ^{26}Al and ^{53}Mn abundances for bulk meteorite samples corresponding to ^{26}Al/^{27}Al $\leqslant 6 \times 10^{-6}$ and ^{53}Mn/^{55}Mn $\leqslant 9 \times 10^{-6}$, respectively (see also the text; Thrane et al. 2006; Shukolyukov & Lugmair 2006; Moynier et al. 2007; Trinquier et al. 2008). There are no constraints on the ^{10}Be abundance in bulk meteorites; instead, the calculated abundance for ^{10}Be is normalized to the inferred solar initial value (i.e., ^{10}Be/^{9}Be $= 1 \times 10^{-3}$). The range of ratios reflects different assumptions among the models regarding the production cross sections, ^{3}He/H and ^{3}He/^{4}He ratios of the SEP, the steepness (p) of the SEP spectra, and the relative importance of gradual to impulsive SEP events (see Leya et al. 2003; Gounelle et al. 2006; Goswami et al. 2005).

2006; Moynier et al. 2007; Trinquier et al. 2008), i.e., $(^{53}$Mn/^{55}Mn$)_0 \leqslant 9 \times 10^{-6}$. With oxygen as its main target element, ^{10}Be will be co-produced with ^{36}Cl in any late SEP irradiation scenario. However, late addition of ^{10}Be is difficult to detect in bulk meteorites because the small amount of ^{10}B produced by decay of ^{10}Be is likely to be overwhelmed by non-radiogenic ^{10}B (the solar B/Be ratio is $\sim$2). The most sensitive test for the late addition of ^{10}Be is determination of boron-isotope abundances in late-forming secondary phases in CAIs or chondrules (e.g., wadalite or grossular). These measurements have not yet been performed but on the basis of the model presented here, we predict ^{10}Be/^{9}Be ratios exceeding 10^{-4} will be found.

In nearly all cases, the amounts of ^{26}Al and ^{53}Mn produced by SEP irradiation of a solar composition reservoir are significantly greater than the values observed in bulk meteorites (Thrane et al. 2006; Shukolyukov & Lugmair 2006; Moynier et al. 2007; Trinquier et al. 2008), and an irradiation model accounting for ^{36}Cl, ^{26}Al, and ^{53}Mn in a self-consistent manner is difficult to achieve (Figure 4). Only in the case of an extremely high SEP spectra, $p \geqslant 5$, where p is the spectral exponent of the SEP power law (see Gounelle et al. 2006), is a self-consistent solution achievable (Figure 4). If the initial ^{36}Cl abundance, however, was any higher than the assumed value (i.e., ^{36}Cl/^{35}Cl $> 2 \times 10^{-5}$), the problem will be exacerbated. The calculations presented above do not consider any delay between production and delivery of newly synthesized ^{36}Cl to the parent body or dilution of the irradiated product with unirradiated material. The ^{36}Cl abundance assumed for the SLR abundance calculations (Figure 4) is likely a lower limit for the amount produced by late irradiation. Thus, ^{36}Cl production by late-stage SEP irradiation of a reservoir with solar composition would very likely overproduce both ^{26}Al and ^{53}Mn.

Overproduction of ^{26}Al and ^{53}Mn can be avoided if the reservoir irradiated to produce ^{36}Cl was depleted in refractory elements (enriched in volatile elements) relative to a solar composition due to CAI and chondrule formation. In particular, irradiation of a reservoir enriched in chlorine—a primary target element for SEP production of ^{36}Cl—would significantly enhance the production of ^{36}Cl relative to ^{26}Al and ^{53}Mn. During the lifetime of the protoplanetary disk, chlorine is present mainly as HCl gas (Zolotov & Mironenko 2007). It will condense as solid HCl hydrates (HCl$\bullet$3H$_2$O) when temperatures fall below $\sim$160 K and may adhere to mineral grains and water ice particles (Zolotov & Mironenko 2007). SEP irradiation of either an HCl-rich gas or dust particles mantled by HCl hydrates would significantly enhance the production of ^{36}Cl relative to ^{26}Al and ^{53}Mn.

5. ^{36}Cl: WHERE, WHEN, AND HOW

The short half-life of ^{36}Cl requires that ^{36}Cl was incorporated into wadalite within 9×10^5 yr (i.e., three half-lives of ^{36}Cl) following production. This temporal constraint places limits on the location of SEP irradiation in the protoplanetary disk. Most models of SLR production by SEP irradiation assume the irradiation occurs near the co-rotation point of the Sun and the protoplanetary disk, known as the X-point (Shu et al. 2001), during the earliest stages of the solar system evolution when the Sun was a young (class 0) or accreting (class I) protostar. However, radial transport of material in the latter stages of the protoplanetary disk (when ^{36}Cl was produced) is inefficient (Ciesla 2007), and we infer that formation of ^{36}Cl must have occurred adjacent to the region in which the CV chondrite parent asteroid accreted. Thus, we propose that ^{36}Cl was largely produced by late-stage SEP irradiation of a volatile-rich reservoir in an optically thin protoplanetary disk while the Sun was a weak T Tauri star. Subsequently, ^{36}Cl accreted into the CV chondrite asteroid together with condensed water ices and was incorporated into secondary, chlorine-rich minerals, wadalite and sodalite, during prolonged parent body alteration. Delivery of chlorine as a component of water ice is consistent with the positive correlation between the chlorine content in chondrites and the degree of aqueous alteration (Zolotov & Mironenko 2007).

REFERENCES

Boss, A. P. 2008, Earth Planet. Sci. Lett., 268, 102
Catanzaro, E. J., Murphy, T. J., Garner, E. L., & Shields, W. R. 1966, J. Res. Natl Bur. Stand., 70a, 453
Ciesla, F. J. 2007, Science, 318, 613
Ding, T., Valkiers, S., Kipphardt, H., De Bievre, P., Taylor, P. D. P., Gonfiantini, R., & Krouse, R. 2001, Geochim. Cosmochim. Acta, 65, 2433
Feigelson, E. D., Garmire, G. P., & Pravdo, S. H. 2002, ApJ, 572, 335
Goswami, J. N., Marhas, K. K., Chaussidon, M., Gounelle, M., & Meyer, B. S. 2005, in ASP Conf. Ser. 341, Chondrites and the Protoplanetary Disk, ed. A. Krot, E. Scott, & B. Reipurth (San Francisco, CA: ASP), 485
Goswami, J. N., Marhas, K. K., & Sahijpal, S. 2001, ApJ, 549, 1151
Gounelle, M., Shu, F. H., Shang, H., Glassgold, A. E., & Rehm, K. E. 2006, ApJ, 640, 1163
Hsu, W., Guan, Y., Leshin, L. A., Ushikubo, T., & Wasserburg, G. J. 2006, ApJ, 640, 525

Huss, G. R., Meyer, B. S., Srinivasan, G., Goswami, J. N., & Sahijpal, S. 2009, Geochim. Cosmochim. Acta, 73, 4922

Ishii, H. A., Krot, A. N., Keil, K., Nagashima, K., Bradley, J. P., Teslich, N., Jacobsen, B., & Yin, Q. 2010, Am. Mineral., 95, 440

Jacobsen, B., Yin, Q.-Z., Moynier, F., Amelin, Y., Krot, A. N., Nagashima, K., Hutcheon, I. D., & Palme, H. 2008, Earth Planet. Sci. Lett., 272, 353

Krot, A. N., Nagashima, K., Hutcheon, I. D., Ishii, H. A., Jacobsen, B., Yin, Q.-Z., Davis, A. M., & Simon, S. B. 2010, Lunar Planet. Sci. Conf., 41, 1406

Leya, I., Halliday, A. N., & Wieler, R. 2003, ApJ, 594, 605

Lin, Y., Guan, Y., Leshin, L. A., Ouyang, Z., & Wang, D. 2005, Proc. Natl Acad. Sci., 102, 1306

McKeegan, K. D., & Davis, A. M. 2003, in Treatise on Geochemistry, Vol. 1, ed. H. D. Holland, K. K. Turekian, & A. M. Davis (Amsterdam: Elsevier), 431

Moynier, F., Yin, Q.-Z., & Jacobsen, B. 2007, ApJ, 671, L181

Nakashima, D., Ott, U., Hoppe, P., & El Goresy, A. 2008, Geochim. Cosmochim. Acta, 72, 6141

Shu, F. H., Shang, H., Gounelle, M., Glassgold, A. E., & Lee, T. 2001, ApJ, 548, 1029

Shukolyukov, A., & Lugmair, G. W. 2006, Earth Planet. Sci. Lett., 250, 200

Thrane, K, Bizzarro, M., & Baker, J. A. 2006, ApJ, 646, L159

Trinquier, A., Birck, J.-L., Allègre, C. J., Göpel, C., & Ulfbeck, D. 2008, Geochim. Cosmochim. Acta, 72, 5146

Ushikubo, T., Guan, Y., Hiyagon, H., Sugiura, N., & Leshin, L. A. 2007, Meteorit. Planet. Sci., 42, 1267

Villeneuve, J., Chaussidon, M., & Libourel, G. 2009, Science, 325, 985

Wasserburg, G. J., Busso, M., Gallino, R., & Nollett, K. M. 2006, Nucl. Phys. A, 777, 5

Zolotov, M. Y., & Mironenko, M. V. 2007, Lunar Planet. Sci. Conf., 38, 2340